

# Controlling the size and shape of gold nanoparticles in fulvic acid colloidal solutions and their optical characterization using SERS

David S. dos Santos, Jr.,<sup>ab</sup> Ramon A. Alvarez-Puebla,<sup>a</sup> Osvaldo N. Oliveira, Jr.<sup>b</sup> and Ricardo F. Aroca<sup>\*a</sup>

Received 3rd May 2005, Accepted 24th May 2005

First published as an Advance Article on the web 15th June 2005

DOI: 10.1039/b506218g

The size and shape of nanoparticles can be controlled by varying the pH and concentration of the fulvic acid (FA) colloidal solution. FA thin solid films with embedded Au nanoparticles have been fabricated, and their optical field enhancing properties tested in surface-enhanced Raman scattering (SERS). High-resolution transmission electron microscopy data indicated that the size of nanoparticles ranges from 4 to 15 nm for films obtained at pH 11 and 8. At pH 5, however, hexagonal and triangular particles of  $\sim 50$  nm and truncated triangles of  $\sim 200$  nm are produced with a high concentration of fulvic acid ( $250 \text{ mg L}^{-1}$ ). The number and size of truncated triangles can be diminished by decreasing the concentration of FA in the colloidal solution. This unprecedented control of size and shape was preserved in thin solid FA films embedding the gold nanoparticles. The plasmon-assisted enhancing optical properties are demonstrated by SERS of 2-naphthalenethiol, an analyte with a well defined SERS spectrum.

## Introduction

The precise control of the size and shape of metallic nanoparticles is one of the main objectives to further exploit their unique chemical and physical properties in catalytic, biological and sensing applications.<sup>1–4</sup> Since Faraday's pioneering work,<sup>5</sup> several methods have been developed to synthesize gold nanoparticles, including physical methods such as metal evaporation,<sup>6</sup> and chemical methods based on the reduction of ionic gold in liquid systems.<sup>7,8</sup> The main stream of published work on the fabrication and characterization of metal nanoparticles involves chemical methods, from which it has been inferred that the shape, size, size distribution, and stability of nanoparticles depends on specific preparation methods, especially on the reducing agents used. The use of mild or weak step-by-step reduction facilitates the seeding formation and growth in aqueous solutions. Given the redox potential of Au(III), various reducing agents may be used, for example, borohydrides, amines, alcohols, carboxylic acids, polysaccharides, fungi<sup>9</sup> and humic substances.<sup>10</sup> Chemical methods may be tuned to deliver specific sizes and shapes for the nanoparticles, and therefore the main challenge now is to develop the analytical protocol leading to nanoparticles of different sizes and shapes in a reproducible way.<sup>11</sup> In summary, chemical methods use the salt of the metal, a reducing and a protective agent dissolved in water or any other appropriate solvent. In this context, the use of macromolecules seems to be advantageous, since they offer control over the rate of the oxidation process, and may act both as the reducing and protecting agents.<sup>12</sup> In this paper we demonstrate the use of fulvic acid

(FA) in the synthesis of gold nanoparticles, where unprecedented control of particle size and shape is achieved by varying the experimental conditions. Fulvic acids are the most water-soluble fractions of humic substances (HS), which are the main components of organic matter of soils and sediments in waters.<sup>13,14</sup> HS play an important role in the accumulation and bioavailability of metals in nature.<sup>15,16</sup> There are several independent reports dealing with the uptake of metallic gold and reduction of gold ions in the environment. The reduction of gold ions by HS seems to be a more favourable process than the adsorption of metallic gold; however, this issue is still under discussion.<sup>17</sup> The formation of colloidal gold particles by humic substances was observed by Machesky *et al.* in his studies of possible mechanisms of interaction of Au with HS in the natural environment.<sup>10,18</sup> In the current study, gold nanoparticles of different shapes and sizes are produced through the reaction of FA and gold tetrachloric acid. FA–Au films prepared by casting are used as substrates for analytical applications in surface-enhanced Raman scattering (SERS).

## Experimental

FA was extracted from a commercial humic substance by Acros Organics (Geel, Belgium). It was fractionated by adjusting the pH of a  $40 \text{ g L}^{-1}$  HS solution to 1.0. FA was then purified using a XAD-8 resin column, and converted to the protonated form by passing it through a proton-saturated resin, then freeze-drying it, in accordance with the procedure proposed by the International Humic Substance Society (IHSS).<sup>19</sup> The resulting material was characterized by means of CHNS, UV–vis, FTIR and acidic properties by chemical methods. The results have been previously reported.<sup>20</sup>

Gold nanoparticles were produced by mixing 20 mL of 0.01% HAuCl<sub>4</sub> (Aldrich) water solution with an equal volume of fulvic acid solution at three different pHs (5, 8 and 11) and

<sup>a</sup>Materials and Surface Science Group, School of Physical Sciences, University of Windsor, Windsor, ON, Canada N9B 3P4.

E-mail: rroca1@cogeco.ca; Fax: 1 519 9737098;

Tel: 1 519 2533000 (ext. 3528)

<sup>b</sup>Instituto de Física de São Carlos, Universidade de São Paulo, CP-369 13560-970, São Carlos, SP, Brazil

concentrations (25, 100 and 250 mg L<sup>-1</sup>). The plasmon absorption of the gold nanoparticles was monitored for various times of reaction, by recording the electronic absorption spectra. FA films were prepared by casting 30 μL of the

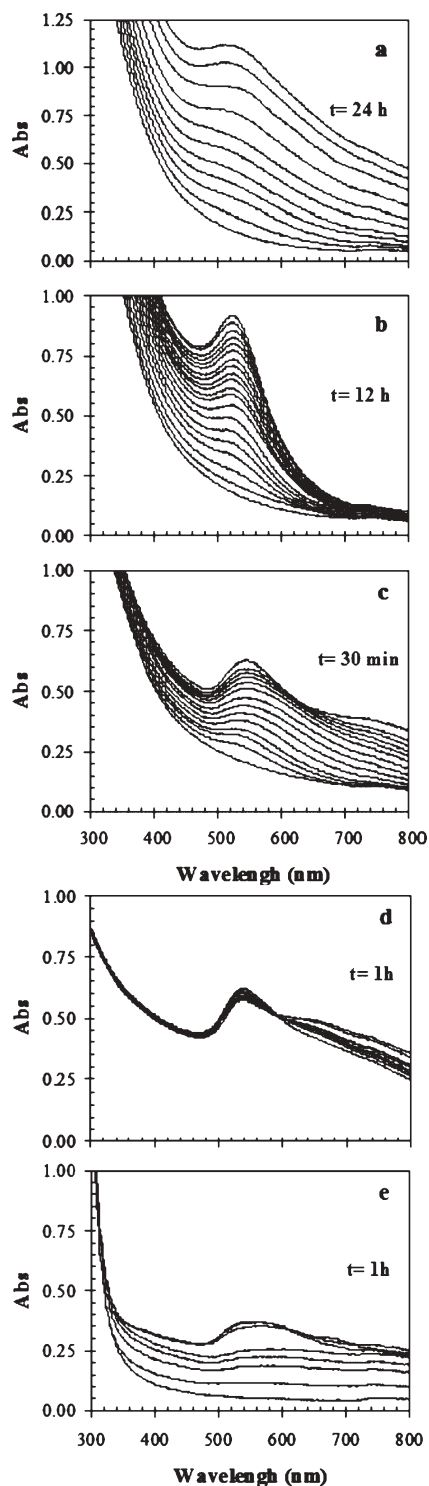


**Fig. 1** Dipolar plasmon absorption recorded during the synthesis of the gold nanoparticles with FA solutions of (a) 250 mg L<sup>-1</sup> at pH 11, (b) 250 mg L<sup>-1</sup> at pH 8, (c) 250 mg L<sup>-1</sup> at pH 5, (d) 100 mg L<sup>-1</sup> at pH 5, and (e) 25 mg L<sup>-1</sup> at pH 5. In every set of spectra, the time after which every spectrum was recorded is indicated.

FA-Au solutions at pH values of 5, 8, and 11, on glass (7059 Corning) slides.

Gold islands films of 9 nm mass thickness were prepared in a Balzers BSV 080 glow discharge evaporation unit. The metal films were deposited on preheated (200 °C) glass slides. During film deposition the background pressure was maintained at  $\sim 10^{-6}$  Torr, and the deposition rate ( $0.5 \text{ \AA s}^{-1}$ ) was monitored using an XTC Inficon quartz crystal oscillator.<sup>21</sup> Gold citrate colloids were prepared following the procedures of Tolaieb *et al.*<sup>22</sup> The process for casting these colloids was analogous to that adopted for fulvic-gold films.

UV-Visible extinction spectra (300–1100 nm) of the gold suspensions, island films and FA films were recorded with a Varian Cary 50 UV-visible spectrophotometer. TEM analysis was performed with a Philips CM12 operating at 120 keV.<sup>23</sup> AFM (Digital Instruments NanoScope IV) topographical measurements were performed in the tapping mode with a silicon cantilever (NSC 14 model, Ultrasharp) operating at a resonant frequency of 249 kHz. Images were collected with high resolution (512 samples per line) at a scan rate of 0.5 Hz. The data were collected under ambient conditions, and each scan was duplicated to ensure that any features observed were reproducible.<sup>24</sup> All samples for SERS measurements were prepared by casting 10 μL of a 10<sup>-4</sup> M ethanol solution of 2-naphthalenethiol (Aldrich) onto FA films. The approximate total area of the casting was 10 mm<sup>2</sup>, while the spatial resolution of SERS microscopy was 1 μm<sup>2</sup>. SERS spectra were collected with a Renishaw Invia system, equipped with Peltier CCD detectors and a Leica microscope. The spectrographs use 1800 g mm<sup>-1</sup> gratings with additional band-pass filter optics. Excitation lines of 488, 514.5, 633, and 785 nm were

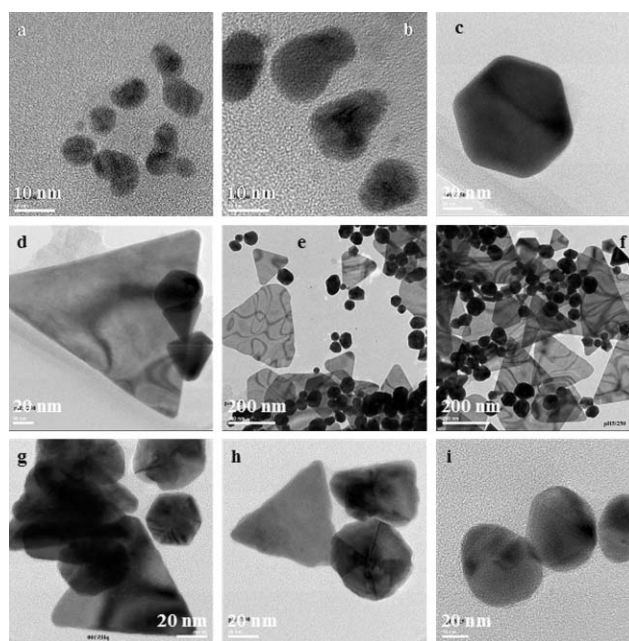


**Fig. 2** High resolution TEM images for gold nanoparticles synthesized with FA solutions of (a) 250 mg L<sup>-1</sup> at pH 11, (b) 250 mg L<sup>-1</sup> at pH 8, (c–f) 250 mg L<sup>-1</sup> at pH 5, (g,h) 100 mg L<sup>-1</sup> at pH 5, and (i) 25 mg L<sup>-1</sup> at pH 5.

used. Spectra were collected in Renishaw's extended collection mode, with accumulation times of 10 s.

## Results and discussion

As Fig. 1 illustrates, both pH and concentration of the solutions affected the dipolar plasmon absorption. The synthesis of Au colloids at pH 11 with  $250 \text{ mg L}^{-1}$  FA solution (Fig. 1a) leads to a spectrum with a broad peak centered at 502 nm, which shifts to a narrower one at 510 nm when the pH of the FA solution is decreased to 8 (Fig. 1b). In both cases, absorption increases slowly with the reaction time. When the solution pH is 5, the spectra show a shift in the maximum to 546 nm and the appearance of a new peak at 750 nm (Fig. 1c). In order to test the effect of FA concentration, the concentration of the solution was reduced to 100 and  $25 \text{ mg L}^{-1}$  of FA. When the gold is treated with these diluted solutions at alkaline pH, there is no reduction observed after two weeks of monitoring the reaction. However, when the solution was at pH 5, the electronic spectra showed surface plasmon peaks that were shifted to 537 nm with  $100 \text{ mg L}^{-1}$  (Fig. 1d) and 530 nm with  $25 \text{ mg L}^{-1}$  (Fig. 1e). The spectrum of the colloids

produced with the  $100 \text{ mg L}^{-1}$  solution also displayed a shoulder placed at 641 nm. The kinetics of the reactions at pH 5 is faster than those at alkaline pH and the reaction rate increases with the FA concentration.

In order to study the effect of pH and FA concentration on the shape and size of the gold nanoparticles, we employed high-resolution transmission electron microscopy (HRTEM). Fig. 2 shows that the size of the colloidal particles increases as the pH decreases. For pH 11 the size of the nanoparticles is in the range from 4 to 10 nm (Fig. 2a). The colloids at pH 8 produce a slightly larger size range, from 10 to 15 nm (Fig. 2b). At pH 5 the micrographs show great differences as a function of the concentration of FA. When the concentration is  $250 \text{ mg L}^{-1}$  FA (Fig. 2c–f), the micrographs show two different sizes: hexagonal and triangular particles of  $\sim 50 \text{ nm}$  and truncated triangles of  $\sim 200 \text{ nm}$ . The number and size of truncated triangles decrease with a concentration of  $100 \text{ mg L}^{-1}$  FA (Fig. 2g,h) and disappear at concentrations of  $25 \text{ mg L}^{-1}$  (Fig. 2i), which can also be inferred from the plasmon absorption spectra (Fig. 1c–e). The size of the nanoparticles decreases with concentration of FA. In the range from 100 to  $25 \text{ mg L}^{-1}$  FA the particle size is  $\sim 40 \text{ nm}$ , and, at

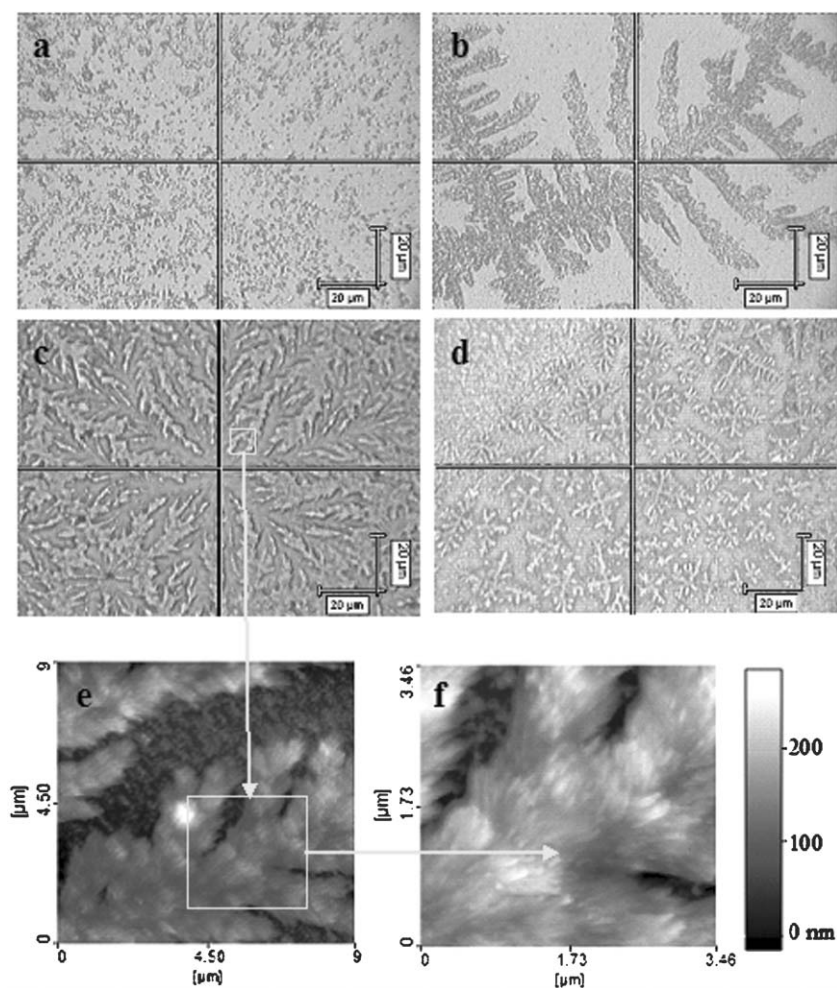


**Fig. 3** Optical images of gold fulvic films produced by casting Au–FA colloidal solutions at (a) pH 5, (b) pH 8, and (c) pH 11. (d) Represents the gold-fulvic film at pH 11 after being exposed to 2-naphthalenethiol solution. (e,f) Show the AFM micrographies of one of the fractal branches of the Au–fulvic films at pH 11.

the same time, with the lowering of the FA concentration, the non-spherical geometrical shapes completely disappear, giving rise to quasi-spherical particles.

In summary, by controlling the pH and the concentration of FA, nanoparticles of distinctly different sizes and different shapes can be produced. The reaction kinetics are also strongly dependent on the pH of the solution, and the reaction rate increases with decreasing pHs for a given FA concentration. For instance, using a 250 mg L<sup>-1</sup> FA solution at room temperature and pH 5, an increase in the plasmon absorption is detected after 1 h, and the reaction is completed within 30 h. In contrast, the same reaction carried out at pH 8 or pH 11 requires, respectively, 132 or 240 h for completion. The reaction rate is probably conditioned by gold speciation<sup>10,25</sup> and ionization of carboxylic groups.<sup>26</sup> The rate of ionization of carboxylic and phenolic acidic groups increases at higher pH, giving rise to more negatively charged molecules.<sup>14</sup> On the other hand, according to the speciation diagram for Au(III) in the presence of chloride<sup>10</sup>, the predominant gold species in the pH range of 11–8 is Au(OH)<sub>4</sub><sup>-</sup>. Thus, the increase in the solution pH leads to an increase in the electrostatic repulsion between the Au(III) complex ions and the fulvic acid macromolecules, causing the reaction kinetics to slow down. The increase in size as the pH decreases may also be related to the decrease of the molecular charge of the fulvic macromolecules that protect the metal colloids, due to a lower ionization of the acidic groups. The lower ionic strength of the solution of the complex may facilitate the interaction between nanoparticles and thereby the aggregation. In addition, the particle size increases with the FA concentration due to the thermodynamic driving force whereby large clusters grow at the expense of small clusters, resulting in ripening according to Ostwald's rule.<sup>27,28</sup> This latter effect leads to the triangle and hexagonal shapes which seem thinner than the quasi-spherical particles obtained at lower concentrations (25 mg L<sup>-1</sup>). Such structures have already been observed for gold nanoparticles synthesized with aspartate, polypeptides and salicylic acid.<sup>29–31</sup> Our own results are unique since the size control is achieved by varying the pH and FA concentration.

The control of size and shape of gold nanoparticles that can be used embedded in fulvic acid films opens the way for a variety of applications. For example, these films can serve as substrates for surface-enhanced Raman scattering (SERS),<sup>32</sup> as we shall show here. First, we employ SERS to characterize the fabricated nanoparticles. The substrates were prepared by casting 30 μL of FA–Au solution onto glass slides (7059 Corning), followed by air-drying. The optical microscopy and AFM of the cast films revealed distinct morphologies according to the method of preparation. Cast fulvic acid films from solutions with different pHs are shown in Fig. 3. At pH 5 fulvic films form small aggregates (Fig. 3a). At pH 8 and 11 (Fig. 3b and 3c), a fractal-like morphology is observed. These fractal-like structures, preserved down to the sub-micrometer range for pH 11 as shown in the AFM images (Fig. 3e and 3f), are probably formed because of the ionized acidic groups, which induce organization in a fractal fashion.<sup>20</sup> The molecular probe (2-naphthalenethiol, 2NT) was delivered in 5 μL of a 10<sup>-3</sup> M ethanolic solution of the organic contaminant, dropped and air-dried. The interaction of the 2NT

solution with the fulvic embedded gold nanoparticles seems to locally perturb the fractal-like structure formed at any pH. However, the fulvic film generated from the pH 11 solution reorganizes itself again as a fractal-like structure but with a different pattern (Fig. 3d).

SERS spectra were recorded using several laser lines (488, 514, 633 and 785 nm). However, the best SERS results were obtained with the 785 nm laser line. The fundamental vibrational modes of 2NT were assigned and discussed in a previous report<sup>33</sup>. The corresponding SERS spectrum was also characterized, and it is the characteristic pattern of SERS for the 2NT analyte that is used here as a probe to test the optical enhancing properties of the fulvic–gold films. For comparison, and as a reference for SERS, the spectra of 2NT on citrate–gold colloids, and on a gold island film of 9 nm mass thickness are also given in Fig. 4. All the spectra were recorded with the same experimental conditions with an objective that illuminates an area of *ca.* 1 μm<sup>2</sup>. The characteristic SERS spectrum of 2NT is clearly recognized on all the SERS active substrates. Fulvic acid films containing gold nanoparticles prepared from solutions at pH 11 do not enhance the inelastic scattering of 2NT. The enhancement of the Raman scattering increases for Au–FA films obtained from solutions at lower pHs. There is already considerable enhancement for the Au–FA films prepared at pH 8, but the best enhancement is attained from Au–fulvic acid film cast from a pH 5 solution. At this pH, the enhancement decreases with the fulvic acid concentration. Notably, at pH 5 fulvic films favor the formation of small aggregates that increases the probability for highly localized plasmon excitations, hot-spots, believed to be responsible for the huge amplifications seen in single molecule SERS.<sup>34</sup> The

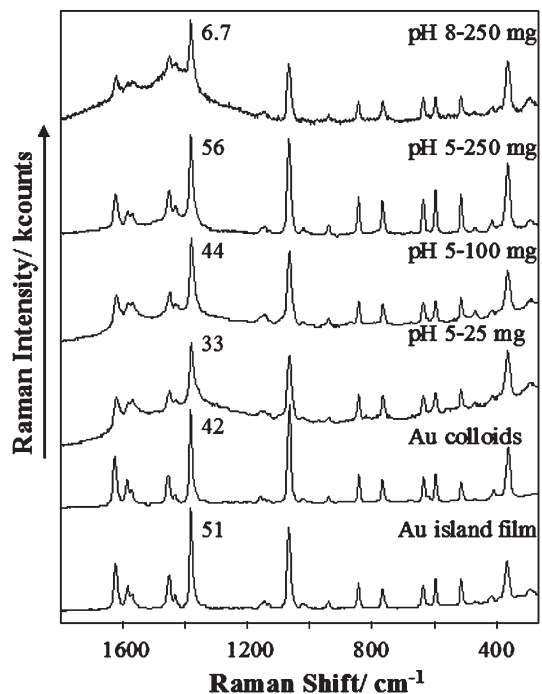


Fig. 4 SERS spectra of 2-naphthalenethiol on gold–fulvic films, citrate–gold colloids cast on a glass slide, and gold island film of 9 nm of thickness. The number of kilocounts for the most intense band of the analyte is shown in each spectrum.

differences in the enhancement may also be affected by the extension of the adsorption of 2NT. The highly charged FA formed at high pH values may hinder the adsorption of 2NT onto the gold nanoparticles. However, the observed SERS spectra show that samples containing a higher number of truncated triangles give a stronger signal. The enhancement factor provided by the Au-FA films fabricated at pH 5 are comparable or even better than that obtained by using the usual substrates (island films or colloids).

## Conclusions

The fabrication of gold nanoparticles of different sizes and shapes is mediated by the pH of the colloidal solution, which provides control of the reaction kinetics, and by the fulvic acid concentration. Furthermore, the colloidal Au-fulvic acid stock solutions are shown to form cast films embedding gold nanoparticles. The optical properties of cast films formed were used as SERS substrates. The enhanced Raman scattering spectrum of 2-naphthalenethiol adsorbed onto an Au-FA film was obtained and compared with SERS recorded on Au colloids and Ag island films. The enhancement factor provided by the Au-FA films is similar or even better than that obtained by using the usual substrates (island films or colloids).

## Acknowledgements

Financial support from NSERC (Canada), Fapesp and CNPq (Brazil) is gratefully acknowledged.

## References

- 1 A. N. Shipway, E. Katz and I. Willner, *ChemPhysChem*, 2000, **1**, 18–52.
- 2 S. Link and M. A. El-Sayed, *Int. Rev. Phys. Chem.*, 2000, **19**, 409–453.
- 3 K. L. Kelly, E. Coronado, L. L. Zhao and G. C. Schatz, *J. Phys. Chem. B*, 2003, **107**, 668–677.
- 4 *Metal Nanoparticles. Synthesis, Characterization and Applications*, ed. D. L. Feldheim and C. A. Foss, Marcel Dekker, Inc., New York, 2002.
- 5 M. Faraday, *Philos. Trans. R. Soc. London*, 1857, **147**, 145.
- 6 R. Blessing and H. Pagnia, *Thin Solid Films*, 1978, **52**, 333–341.
- 7 J. Turkevich, P. L. Stevenson and J. Hillier, *Discuss. Faraday Soc.*, 1951, **11**, 55.
- 8 G. Frens, *Nature*, 1973, **241**, 20–22.
- 9 M.-C. Daniel and D. Astruc, *Chem. Rev.*, 2004, **104**, 293–346.
- 10 M. L. Machesky, W. O. Andrade and A. W. Rose, *Chem. Geol.*, 1992, **102**, 53–71.
- 11 L. M. Liz-Marzan, *Mater. Today*, 2004, **7**, 26–31.
- 12 N. Toshima and T. Yonezawa, *New J. Chem.*, 1998, **22**, 1179–1201.
- 13 E. Tipping, *Cation Binding by Humic Substances*, Cambridge University Press, Cambridge, 2002.
- 14 F. J. Stevenson, *Humus Chemistry: Genesis, Composition and Reactions*, John Wiley & Sons, New York, 1994.
- 15 R. A. Alvarez-Puebla, C. Valenzuela-Calahorra and J. J. Garrido, *Langmuir*, 2004, **20**, 3657–3664.
- 16 R. A. Alvarez-Puebla, C. Valenzuela-Calahorra and J. J. Garrido, *J. Colloid Interface Sci.*, 2004, **277**, 55–61.
- 17 S. A. Wood, *Ore Geol. Rev.*, 1996, **11**, 1–31.
- 18 W. O. Andrade, M. L. Machesky and A. W. Rose, *J. Geochem. Explor.*, 1991, **40**, 95–114.
- 19 R. S. Swift, in *Method of Soil Science Analysis: Chemical Methods. Part 3*, ed. D. L. Sparks, Soil Science Society of America, Madison, WI, 1996, pp. 1011–1069.
- 20 R. A. Alvarez-Puebla, J. J. Garrido and R. F. Aroca, *Anal. Chem.*, 2004, **76**, 7118–7125.
- 21 P. J. G. Goulet, N. P. W. Pieczonka and R. F. Aroca, *Anal. Chem.*, 2003, **75**, 1918–1923.
- 22 B. Tolaieb, C. J. L. Constantino and R. F. Aroca, *Analyst*, 2004, **129**, 337–341.
- 23 Z. Yao, N. Braidy, G. A. Botton and A. Adronov, *J. Am. Chem. Soc.*, 2003, **125**, 16015–16024.
- 24 L. Gaffo, C. J. L. Constantino, W. C. Moreira, R. F. Aroca and O. N. Oliveira, Jr., *Langmuir*, 2002, **18**, 3561–3566.
- 25 F. Burriel, F. Lucena, S. Arribas and J. Hernandez, *Química Analítica Cualitativa*, Paraninfo, Madrid, 1998.
- 26 S. C. B. Myneni, J. T. Brown, G. A. Martinez and W. Meyer-Ilse, *Science*, 1999, **286**, 1335–1337.
- 27 C. N. R. Rao and J. Gopalakrishnan, *New Directions in Solid State Chemistry*, Cambridge University Press, Cambridge, 1997.
- 28 Y. Sun and Y. Xia, *Adv. Mater.*, 2003, **15**, 695–699.
- 29 S. Brown, M. Sarikaya and E. Johnson, *J. Mol. Biol.*, 2000, **299**, 725–735.
- 30 N. Malikova, I. Pastoriza-Santos, M. Schierhorn, N. A. Kotov and L. M. Liz-Marzan, *Langmuir*, 2002, **18**, 3694–3697.
- 31 Y. Shao, Y. Jin and S. Dong, *Chem. Commun.*, 2004, 1104–1105.
- 32 R. K. Chang and T. E. Furtak, *Surface Enhanced Raman Scattering*; Plenum Press, New York, 1982.
- 33 R. A. Alvarez-Puebla, D. S. dos Santos, Jr. and R. F. Aroca, *Analyst*, 2004, **129**, 1251–1256.
- 34 E. C. Le Ru and P. G. Etchegoin, *Chem. Phys. Lett.*, 2004, **396**, 393–397.